AMERICAN SOCIETY FOR MICROBIOLOGY | Infection and Immunity®

CELLULAR MICROBIOLOGY: PATHOGEN-HOST CELL MOLECULAR INTERACTIONS

Staphylococcus aureus and *Acinetobacter baumannii* Inhibit Osseointegration of Orthopedic Implants

Hyonmin Choe,[a,b] Joscelyn M. Tatro,[a] Bryan S. Hausman,[a] Kristine M. Hujer,[c] Steve H. Marshall,[c] Ozan Akkus,[d] Phillip N. Rather,[e,f] Zhenghong Lee,[g] Robert A. Bonomo,[c,h,i,j,k,l,m] Edward M. Greenfield[a,n]

[a]Department of Orthopaedics, Case Western Reserve University, Cleveland, Ohio, USA
[b]Department of Orthopaedics, Yokohama City University, Yokohama, Kanagawa, Japan
[c]CWRU–Cleveland VAMC Center for Antimicrobial Resistance and Epidemiology (Case VA CARES), Cleveland, Ohio, USA
[d]Department of Mechanical Engineering, Case Western Reserve University, Cleveland, Ohio, USA
[e]Department of Microbiology and Immunology, Emory University School of Medicine, Atlanta, Georgia, USA
[f]Research Service, Atlanta Veterans Affairs Medical Center, Decatur, Georgia, USA
[g]Department of Radiology, Case Western Reserve University, Cleveland, Ohio, USA
[h]Medical Service and GRECC, Louis Stokes Cleveland Department of Veterans Affairs Medical Center, Cleveland, Ohio, USA
[i]Department of Medicine, Case Western Reserve University School of Medicine, Cleveland, Ohio, USA
[j]Department of Pharmacology, Case Western Reserve University School of Medicine, Cleveland, Ohio, USA
[k]Department of Molecular Biology and Microbiology, Case Western Reserve University School of Medicine, Cleveland, Ohio, USA
[l]Department of Biochemistry, Case Western Reserve University School of Medicine, Cleveland, Ohio, USA
[m]Center for Proteomics and Bioinformatics, Case Western Reserve University School of Medicine, Cleveland, Ohio, USA
[n]Department of Orthopaedic Surgery, Indiana University School of Medicine, Indianapolis, Indiana, USA

ABSTRACT Bacterial infections routinely cause inflammation and thereby impair osseointegration of orthopedic implants. *Acinetobacter* spp., which cause osteomyelitis following trauma, on or off the battlefield, were, however, reported to cause neither osteomyelitis nor osteolysis in rodents. We therefore compared the effects of *Acinetobacter* strain M2 to those of *Staphylococcus aureus* in a murine implant infection model. Sterile implants and implants with adherent bacteria were inserted in the femur of mice. Bacterial burden, levels of proinflammatory cytokines, and osseointegration were measured. All infections were localized to the implant site. Infection with either *S. aureus* or *Acinetobacter* strain M2 increased the levels of proinflammatory cytokines and the chemokine CCL2 in the surrounding femurs, inhibited bone formation around the implant, and caused loss of the surrounding cortical bone, leading to decreases in both histomorphometric and biomechanical measures of osseointegration. Genetic deletion of TLR2 and TLR4 from the mice partially reduced the effects of *Acinetobacter* strain M2 on osseointegration but did not alter the effects of *S. aureus*. This is the first report that *Acinetobacter* spp. impair osseointegration of orthopedic implants in mice, and the murine model developed for this study will be useful for future efforts to clarify the mechanism of implant failure due to *Acinetobacter* spp. and to assess novel diagnostic tools or therapeutic agents.

KEYWORDS *Acinetobacter*, implant infection, *Staphylococcus*, bioluminescence, osseointegration

Implant infection is one of the most difficult orthopedic complications, as progressive inflammation leads to osteolysis, reduced osteogenesis, impaired osseointegration, and implant loosening (1). This process is typically initiated by macrophage production of inflammatory cytokines that induce production of RANKL by mesenchymal cells and/or T cells (2–6). RANKL then stimulates differentiation and activity of osteoclasts, myeloid-lineage cells that are responsible for the bone resorption that causes local osteolysis (4–7). The inflammatory cytokines also potently reduce osteogenesis (8–14) and thereby impair

Editor Victor J. Torres, New York University School of Medicine

Address correspondence to Edward M. Greenfield, egreenf@iu.edu.

The authors declare no conflict of interest.

Received 16 December 2021
Accepted 6 January 2022
Accepted manuscript posted online 31 January 2022
Published 17 March 2022

osseointegration (15). Despite the importance of osseointegration to achieve successful outcomes of both orthopedic and dental implants (16, 17), few previous murine infection studies included implant materials that allow osseointegration (18–24).

Staphylococcus aureus is the most common and the best characterized cause of orthopedic implant infections (1). Members of the Gram-negative *Acinetobacter calcoaceticus-Acinetobacter baumannii* complex are an increasingly common cause of osteomyelitis and delayed healing in soldiers with orthopedic battlefield wounds (25–28). Most of those infections appear to be acquired in the hospital (i.e., nosocomial) rather than on the battlefield (28–32). *Acinetobacter* spp. are also becoming increasingly prevalent in hospital-acquired infections in civilians (33). These difficult-to-treat nosocomial infections are facilitated by the ability of *Acinetobacter* spp. to persist on surfaces in health care environments (34) and to aerosolize (35, 36). *Acinetobacter* spp. also frequently acquire multidrug resistance, further complicating clinical outcomes (32, 37–39). Despite growing literature on inflammatory responses to *Acinetobacter* spp. in soft tissues and the bloodstream (33, 40–44), little is known about responses in the skeletal environment other than that some, but not all, *A. baumannii* strains cause osteomyelitis in rats (45, 46) and the report that *A. baumannii* increases bone formation in mice without inducing osteolysis (47). That report is especially surprising given that osteolysis is a typical sequela of osteomyelitis in both human and veterinary medicine (48) and in preclinical research in mice (49).

In this study, we used a bioluminescent *S. aureus*-Xen36 (50, 51) implant infection model based on our murine model of osseointegration (52) to compare the effects of *S. aureus* with the effects of the *Acinetobacter calcoaceticus-A. baumannii* complex. We used *Acinetobacter* strain M2, which was isolated from a hip infection in a civilian setting (53) and recently reclassified from *A. baumannii* to *Acinetobacter nosocomialis* (54). A summary of the study is shown in Figure 1.

RESULTS

Bacterial burden. To establish a murine model of chronic, localized implant infection (Fig. 2A), we first used implants with adherent *S. aureus*-Xen36 that is bioluminescent as long as the bacteria are viable (51). Signs of systemic infection were not detected in any mice. Moreover, the bioluminescence imaging (BLI) signals were seen only in the leg surrounding the implant, demonstrating that infection is localized to the implant site (Fig. 2B). BLI in the high-dose *S. aureus* group increased by 4 h postimplantation and remained stable for 7 days (Fig. 2C). BLI decreased between 7 and 14 days but then stabilized and remained significantly higher than that without bacteria for at least 28 days postimplantation (Fig. 2D). BLI in the low-dose *S. aureus* group was intermediate between that of the other two groups at all tested time points (Fig. 2B and C). The validity of the BLI approach was confirmed by *in vitro* measurements showing that the BLI signals were related in a dose-dependent manner to the number of bacteria either in suspension or adherent to the implants (Fig. 3A and B).

Having established a chronic, localized murine model of implant infection, we measured the bacterial burden surrounding implants that were seeded with *S. aureus* or *Acinetobacter* strain M2 (Fig. 1). Again, signs of systemic infection were not detected in any mice. Numbers of CFU and *luxA* gene copies on implants and in surrounding femurs were increased in the high-dose *S. aureus* group at days 7 and 15 postimplantation, and the low-dose *S. aureus* group showed intermediate levels (Fig. 2E, F, and I to J). Since day 7 measurements of CFU and *luxA* gene copies were performed on the same mice as the BLI measurements (Fig. 2B), we asked whether there were correlations among the results. Quadratic regression analysis (Fig. 3C and D) showed that BLI signals correlate with sums of CFU on implants and in surrounding femurs ($r^2 = 0.71$) or *luxA* gene copies on implants and in surrounding femurs ($r^2 = 0.55$). The bacterial burden was also increased in the high-dose *Acinetobacter* strain M2 group, as assessed by numbers of CFU (Fig. 2G and H) and *adeR* gene copies (Fig. 2K and L). However, low-dose *Acinetobacter* strain M2 failed to establish infections (Fig. 2G, H, and K-L), and the high dose of Acinetobacter strain M2 resulted in lower bacterial burdens than the high dose of *S. aureus* (Fig. 2E to H). We therefore also included a higher inoculum of *Acinetobacter* strain M2 that was prepared by overnight incubation of implants with a high concentration of bacteria, which also consistently induced localized implant infections without inducing any signs of systemic infection (Fig. 2G, H, and K-L).

Interleukin 1β (IL-1β) and IL-6 in femurs surrounding implants were measured as exam-

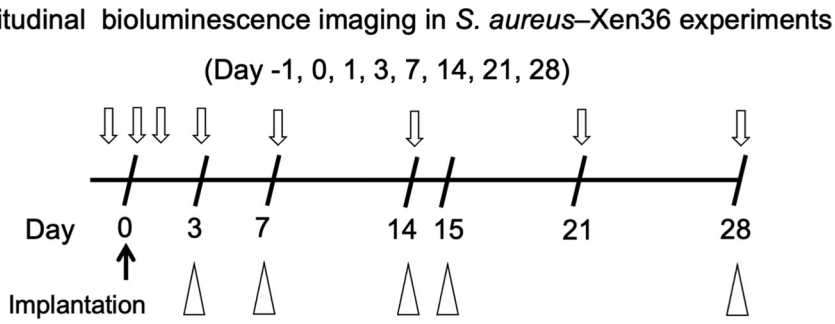

			# of mice at each timepoint		
C57BL/6 mice			**Day7**	**Day 14**	**Day28**
Histomorphometry	*S. aureus*-Xen36 experiment	No bacteria	5	-	5
		Low dose Xen36	5	-	-
		High dose Xen36	5	-	5
	Acinetobacter strain M2 experiment	No bacteria	4	3	-
		Low dose M2	3	-	-
		High dose M2	3	-	-
		Overnight M2	4	4	-
			Day7	**Day 15**	**Day28**
Biomechanical testing followed by measurement of 1. CFU 2. bacterial gene 3. cytokine/chemokine	*S. aureus*-Xen36 experiment	No bacteria	5	10	-
		Low dose Xen36	5	-	-
		High dose Xen36	5	10	-
	Acinetobacter strain M2 experiment	No bacteria	5	10	-
		Low dose M2	5	-	-
		High dose M2	3	-	-
		Overnight M2	12	10	-

FIG 1 Flow chart of the experiments and number of mice enrolled in each experiment.

ples of local inflammatory cytokines (Fig. 1). They were both dose dependently increased by *S. aureus* and *Acinetobacter* strain M2 (Fig. 4A to D). CCL2 was measured as a chemokine that is chemotactic mainly for macrophages (55). CCL2 levels were also increased by *Acinetobacter* strain M2 but were not significantly affected by *S. aureus* (Fig. 4E and F).

Osseointegration. Implants that were not fixed in the femur at the time of euthanasia were recorded as gross integration failures. These failures occurred in 60% of mice in the high-dose *S. aureus* group at both days 15 and 28 (Fig. 5A). Gross integration failures were rare at earlier time points with *S. aureus* and never seen with *Acinetobacter* strain M2 or without bacteria (Fig. 5A).

Consistent with our previous studies (15, 52, 56), osseointegration increased in groups without bacteria between 7 and 15 days postimplantation (Fig. 5B to G). In contrast, biomechanical (Fig. 5B to G) and histomorphometric (Fig. 5H to K) measures of osseointegration were reduced by either type of bacteria (Fig. 5). These results can be seen in images from mice with median histomorphometry results in each group (Fig. 6). Without bacteria, abundant bone formation occurred in contact with implants and between implant threads, and bone resorption was not observed (Fig. 6A to D). In contrast, there was much less bone formation adjacent to implants in the *S. aureus* and *Acinetobacter* strain M2 groups, but both types of bacteria induced periosteal bone formation (Fig. 6E to H). Osteoclasts were observed on the endosteal and periosteal sides

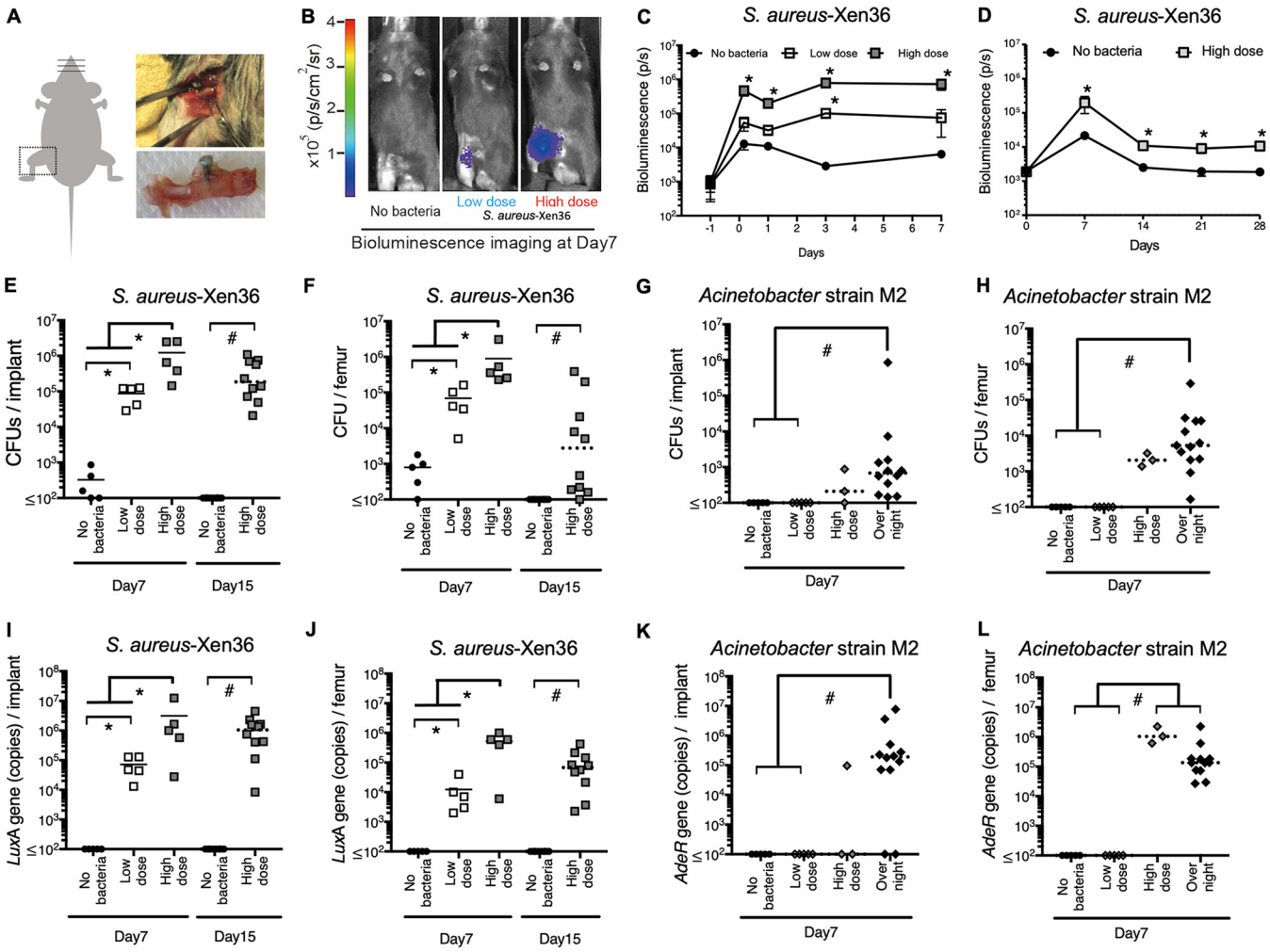

FIG 2 Chronic infection localized to implant site. (A) Diagram depicting implantation in mouse femur. (B) Representative images at 7 days postimplantation from mice with median BLI intensity in groups shown in panel C. (C and D) BLI was measured 1 day preimplantation and 4 h to 7 days (C) or 7 to 28 days (D) postimplantation. $n = 5$ mice/group. *, $P < 0.05$ compared to group without bacteria at the same time point (two-way ANOVA with Bonferroni's *post hoc* analysis). (E to L) The numbers of CFU (E to H) and gene copies (I to L) were measured on implants (E, G, I, K) and in surrounding femurs (F, H, J, L). Solid horizontal bars indicate means for parametric analysis (*, $P < 0.05$). Dashed bars indicate medians for nonparametric analysis (#, $P < 0.05$).

of the original cortex with both types of bacteria (Fig. 6E to G). The combination of periosteal bone formation and endosteal resorption in the absence of endosteal bone formation caused cortical migration away from infected implants (Fig. 6F and H), similarly to the cortical migration that occurs in patients with high-turnover osteoporosis (57).

Effect of TLR2 and TLR4. To gain further understanding of the effects of *Acinetobacter* spp., we compared wild-type mice and mice lacking both TLR2 and TLR4, two of the primary immune receptors for Gram-negative bacteria. Deficiency of both TLRs did not detectably alter osseointegration in the absence of bacteria (Fig. 7A to C) or in the presence of high-dose *S. aureus* (Fig. 7D to F) but partially reduced effects in the *Acinetobacter* strain M2 overnight incubation group (Fig. 7G to I). The effects of TLR deletion are not due to differential bacterial clearance, as the number of bacteria was unaltered at all time points (see Fig. S1A to F in the supplemental material). Moreover, deletion of TLR2 and TLR4 did not detectably affect the levels of CCL2, IL-6, or IL1β in either the absence or presence of infection (Fig. S2).

DISCUSSION

The major goal of the current study was to compare the effects of *S. aureus* with the effects of *Acinetobacter* spp., which have been reported to increase bone formation in mice without inducing osteolysis (46). We first used bioluminescent *S. aureus*-Xen36 (51) to establish a murine model of implant infection based on our previous osseointegration

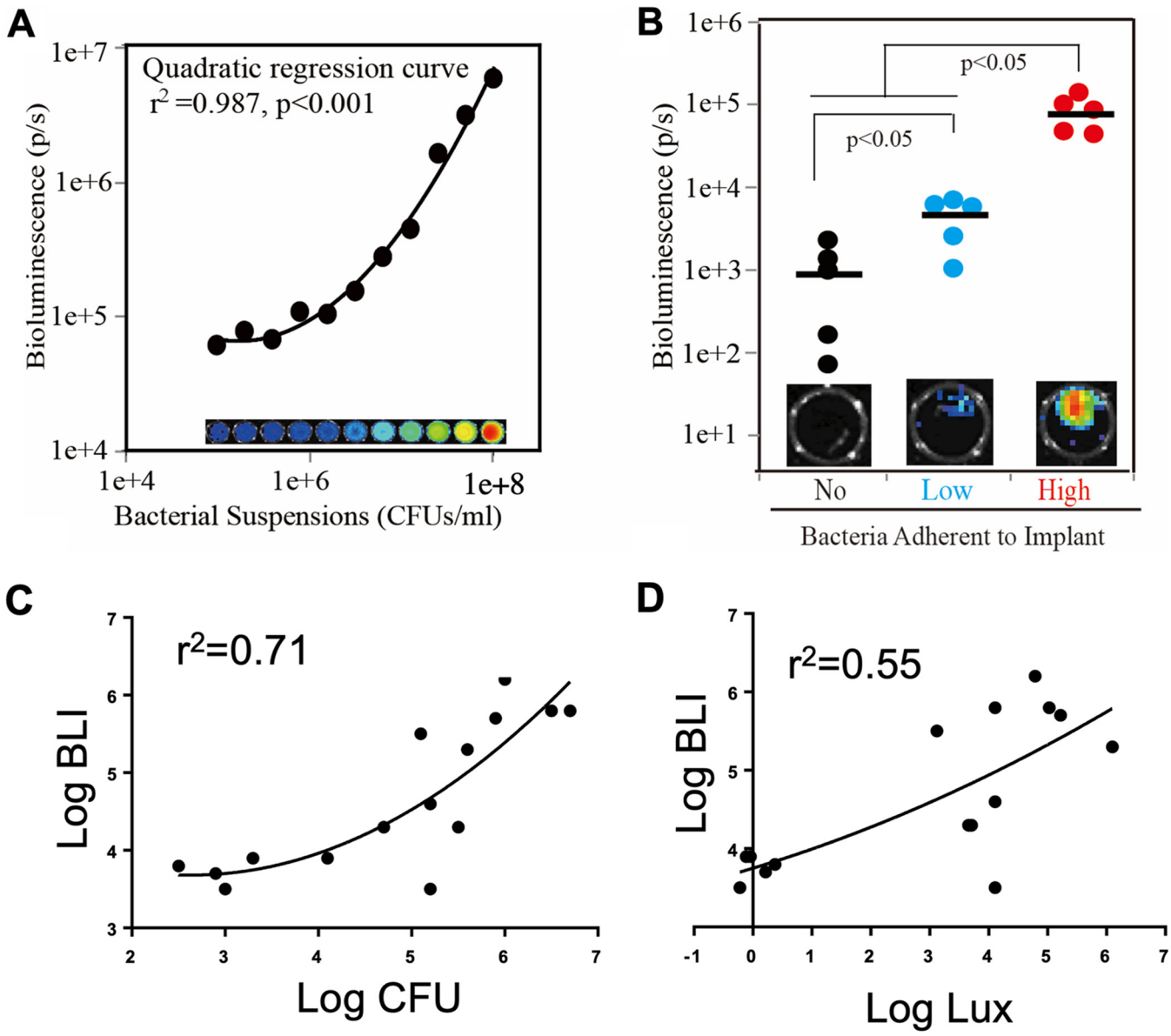

FIG 3 Bioluminescence imaging (BLI) accurately reflects bacterial number *in vitro* and *in vivo*. (A) BLI and CFU were measured in *S. aureus* suspensions after 2-fold serial dilutions. Statistical analysis was by quadratic regression analysis. Inset shows BLI of bacterial suspensions. (B) BLI was measured on implants without insertion into mice. Statistical analysis was by one-way ANOVA with Bonferroni's *post hoc* analysis. Solid horizontal bars indicate means. Inset images are of the implant with BLI closest to the mean. (C and D) BLI was measured in intact mice, and CFU and *luxA* gene copies were measured on implants and in surrounding femurs at day 7. Statistical analysis was by quadratic regression analysis.

model (15, 56). Both *Acinetobacter* strain M2 and *S. aureus* caused local infections on implants and in surrounding bones that were well tolerated and did not induce any systemic signs of infection. Interestingly, *Acinetobacter* strain M2 required a higher initial inoculum to establish infection than *S. aureus*. This may reflect that different strains of *Acinetobacter* exhibit large differences in virulence in rodent models (45, 58–61). In this regard, our infection model uses implants that are preincubated with the bacteria, which likely introduces a higher inoculum than occurs during implant infection in patients. Nonetheless, both *Acinetobacter* strain M2 and *S. aureus* induced production of inflammatory cytokines and impaired histomorphometric and biomechanical measures of osseointegration. The effects of *Acinetobacter* strain M2 and *S. aureus* on osseointegration are likely caused by inflammation that both impaired osteogenesis and induced osteolysis around the implants. Consistent with that possibility, bone loss commonly occurs around infected implants in patients (1) and in previous murine studies of *S. aureus* (21–23, 62).

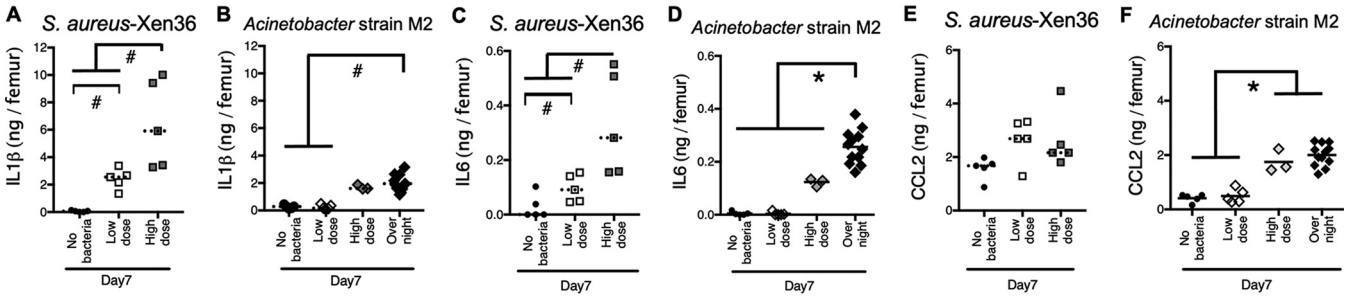

FIG 4 Cytokines and chemokines are increased by implant infection. (A to F) IL-1β (A and B), IL-6 (C and D), and CCL2 (E and F) were measured in femurs surrounding implants at 7 days postimplantation. Solid horizontal bars indicate means for parametric analysis (*, $P < 0.05$). Dashed bars indicate medians for nonparametric analysis (#, $P < 0.05$).

This is the first demonstration in mice that *Acinetobacter* infection impairs osseointegration, a major complication of orthopedic implant infection (1). This finding would not have been predicted based on the report that *A. baumannii* increases osteogenesis in mice without detectably inducing osteolysis (47). This discrepancy could be due to testing different amounts (24) or different strains of *Acinetobacter* (45, 58–61). Consistent with that possibility, some, but not all, *Acinetobacter* strains cause osteomyelitis in rats (45, 46). Alternatively, the discrepancy could be due to a different balance, or different spatiotemporal pattern, between effects on osteogenesis and osteolysis (63). Consistent with that possibility, the micro-computed tomography (uCT) images in reference 47 appear to show a small amount of local osteolysis in combination with robust new bone formation in response to *A. baumannii* compared with a greater amount of osteolysis and more limited, but still substantial, bone formation in response to *S. aureus*. Moreover, we found that both *Acinetobacter* strain M2 and *S. aureus* inhibited osteogenesis on implant surfaces and in the peri-implant region and induced bone resorption on the endosteal and periosteal sides of the original cortex. In contrast, new bone formation was induced on the periosteal side of the original cortex by either type of bacteria. The periosteal new bone formation is a common response to local cortical defects induced by infection (62, 64) or surgical drill holes (63, 65) and also occurs in our osseointegration model in the absence of infection (15, 56).

Impaired osteogenesis and induction of osteolysis around orthopedic implants involve inflammatory processes that include detection of pathogen-associated molecular patterns (PAMPs) by Toll-like receptors (TLRs) (66). Our findings indicate that osseointegration inhibition by *Acinetobacter* spp. depends, in part, on TLR-dependent inflammation. These results are consistent with findings that *Acinetobacter* can activate the innate immune system through TLR2, TLR4, or other pattern recognition receptors, as well as through acyl-homoserine lactones and multiple other virulence factors that act independently of pattern recognition receptors (33, 67, 68).

Macrophage recruitment likely restrains the bacterial burden (9, 69–71) and increases production of inflammatory cytokines that cause inflammatory osteolysis (2, 3, 9, 69) and inhibit osteogenesis and osseointegration (8–14). Consistent with this concept that adverse effects on local bone turnover by bacteria are due primarily to "collateral damage" from the host immune response (72), we found that inflammatory cytokines are increased in bones with infected implants. Macrophages can also contribute to inflammatory bone loss by serving as osteoclast precursors (9, 73), which likely facilitates the bone resorption surrounding infected implants.

Importantly, measurement of bacterial strain-specific bioluminescence and strain-specific genes would not be affected by contaminating bacteria that might have caused misinterpretation of the CFU data. In addition, both genetic and CFU data correlated with bioluminescence imaging of *S. aureus*-Xen36, and the absence, or very low level, of measurable CFU from mice with uninfected implants confirmed the absence of cross-contamination. Measurement of bacterial genes also serves as an example of PCR-based microbiological diagnosis, which is required to document the viable but nonculturable bacteria that can occur in orthopedic infections (74–76).

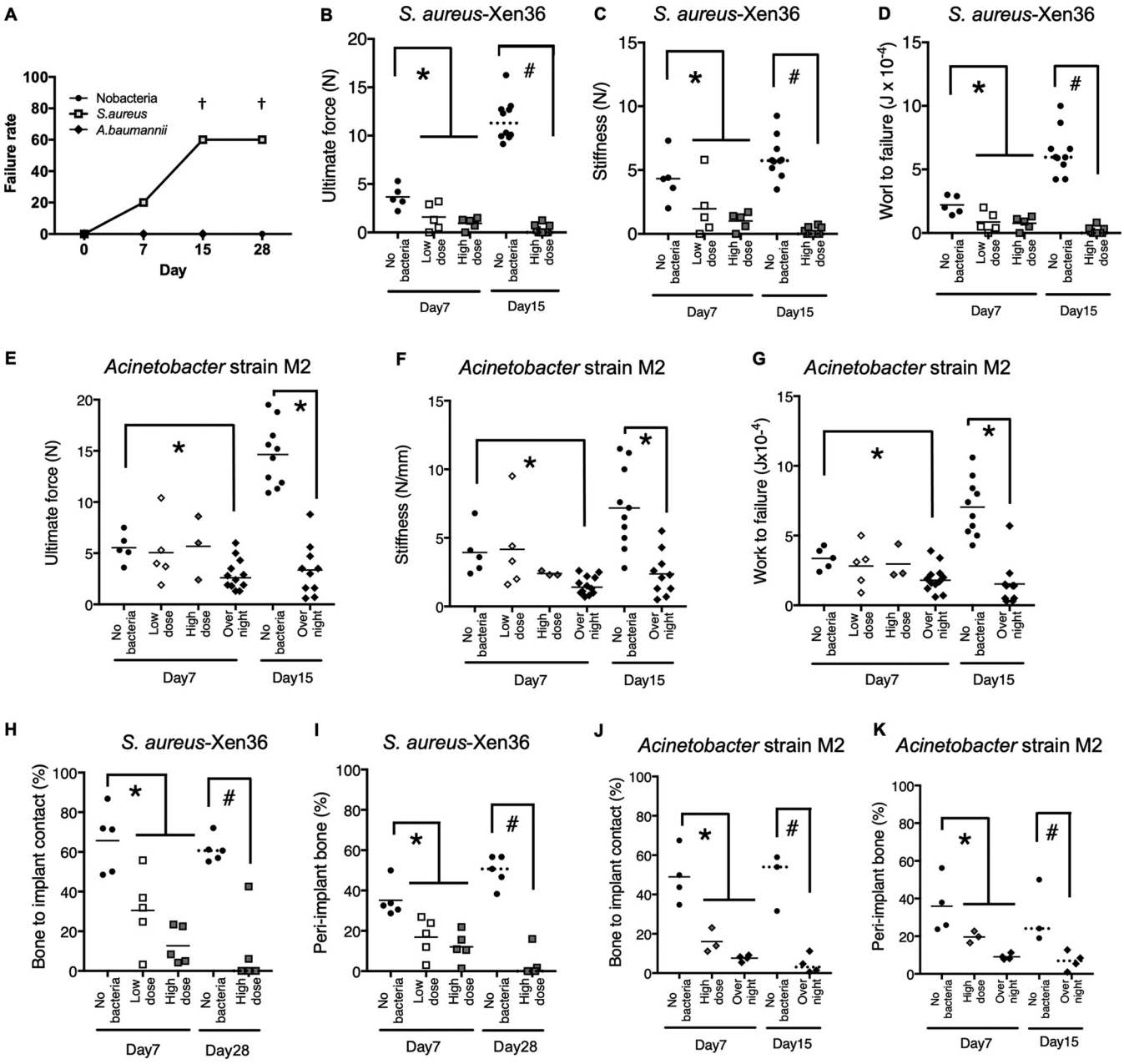

FIG 5 Osseointegration is decreased by implant infection. (A) Implants that were not fixed in the femur at euthanasia were classified as gross integration failures. †, $P < 0.05$ compared to group without bacteria at the same time point ($\chi 2$ test). (B to K) Biomechanical (B to G) and histomorphometric (H to K) measures of osseointegration. Solid horizontal bars indicate means for parametric analysis (*, $P < 0.05$). Dashed bars indicate medians for nonparametric analysis (#, $P < 0.05$).

In conclusion, infection with either *S. aureus* or *Acinetobacter* strain M2 increases inflammatory cytokines and impairs implant osseointegration in our new murine model of orthopedic implant infection. The murine model will also be useful for future studies to clarify the mechanism of implant failure due to *Acinetobacter* spp. and to assess novel diagnostic tools or therapeutic agents.

MATERIALS AND METHODS

Preparation of implants with adherent bacteria. Titanium alloy screw-shaped implants (Ti – 6Al – 4V, 3.2-mm length, 1.0-mm diameter; Antrin Miniature Specialties, Inc., Fallbrook, CA) were autoclaved (15 lb/in^2 and 273°F for 8 min, followed by a 30-min dry cycle) and then rigorously cleaned with five cycles of alternating treatments in alkali ethanol (0.1 N NaOH and 95% ethanol at 32°C) and 25% nitric acid (56). We employed *S. aureus*-Xen36 (Caliper Life Sciences, Hopkinton, MA), which contains a stable copy of the bacterial *luxABCDE* operon and is therefore bioluminescent as long as the bacteria are viable (50, 51), and *Acinetobacter* strain M2 (53).

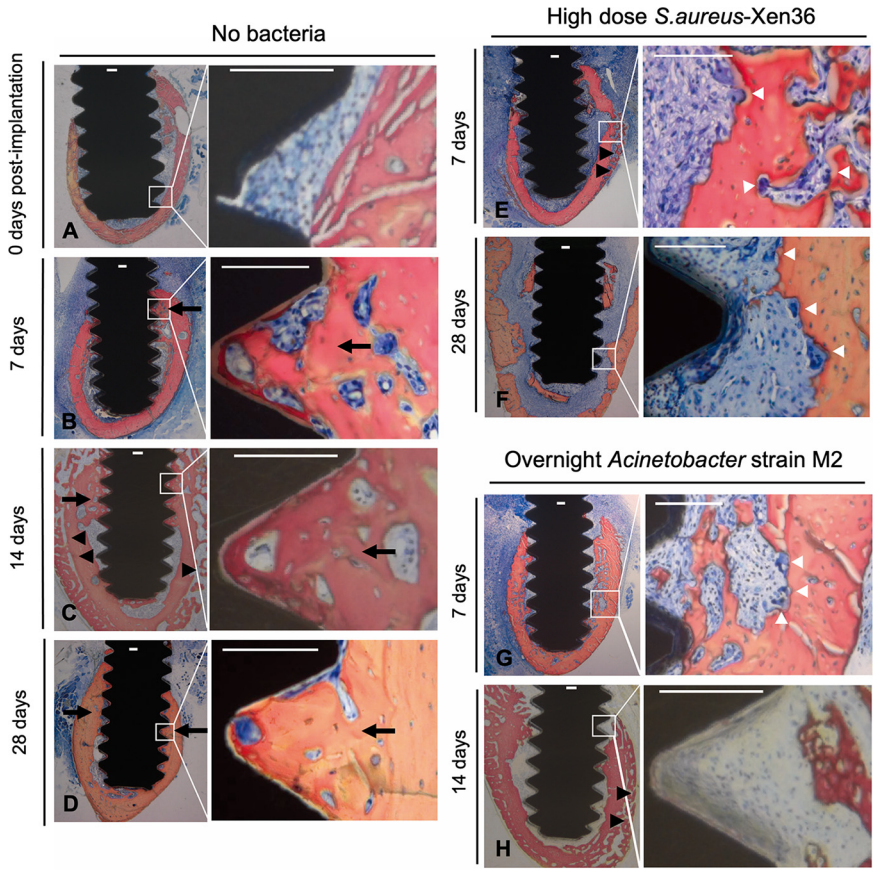

FIG 6 Representative histomorphometry images of osseointegration in the presence and absence of implant infection. (A to H) Representative images from mice with median histomorphometry results in groups without bacteria (A to D), with high-dose *S. aureus* (E and F), or with overnight incubation of *Acinetobacter* strain M2 (G and H). White boxes in low-power images indicate locations of high-power images. All scale bars, 100 μm. Black arrows and arrowheads indicate bone formation on endosteal and periosteal sides of original cortex. White arrowheads indicate osteoclasts.

One day before each implant surgery, a single colony of *S. aureus*-Xen36 or *Acinetobacter* strain M2 was inoculated into 5 mL of lysogenic broth (LB) medium (Fisher Scientific, Fair Lawn, NJ) or Mueller-Hinton broth (MHB) medium (Fisher Scientific, Fair Lawn, NJ), respectively, and incubated at 37°C overnight in a bacterial shaker. Overnight suspensions were diluted 100-fold in LB or MHB medium and incubated at 37°C until early log phase was reached (A_{600}/0.1-cm light path = 0.05; Nanodrop 1000; Fisher Scientific). Those low-concentration bacterial suspensions (1×10^9 to 3×10^9 CFU/mL) were centrifuged (1,500 $\times$ *g*, 5 min) and resuspended in 1/30 volume of LB broth or MHB to obtain high-concentration suspensions (3×10^{10} to 9×10^{10} CFU/mL). The rigorously cleaned implants were incubated with low- or high-concentration bacterial suspensions for 20 min at 37°C with gentle shaking to obtain low- and high-dose implant groups (52). Implants with higher levels of *Acinetobacter* strain M2 were obtained by incubation with high-concentration suspensions for 24 h and are referred to as the overnight incubation group. Implants with adherent bacteria were rinsed 3 times in phosphate-buffered saline (PBS) (pH 7.4) and immediately implanted into mice as described below. Additional implants were simultaneously prepared to measure the adherent CFU as described below. Numbers of adherent *S. aureus*-Xen36 CFU were 2×10^4 to 6×10^4 and 0.5×10^6 to 2×10^6 CFU/implant in low- and high-dose groups, respectively. Numbers of adherent *Acinetobacter* strain M2 CFU were 4×10^5 to 7×10^5, 1×10^6 to 3×10^6, and 1×10^7 to 3×10^7 CFU/implant in low-dose, high-dose, and overnight incubation groups, respectively.

Animal surgery. Wild-type C57BL/6J female mice were purchased from Jackson Laboratory (Bar Harbor, ME). TLR2$^{-/-}$;TLR4$^{-/-}$ mice (77, 78) were gifts from Amy Hise (CWRU Department of Pathology). All procedures were approved by the CWRU Institutional Animal Care and Use Committee. Mice were maintained under specific-pathogen-free conditions with unlimited access to food and water in the CWRU Animal Resource Center, where all procedures were performed. All procedures were approved by the CWRU Institutional Animal Care and Use Committee. Mice were randomized among groups (Fig. 1), anesthetized by intraperitoneal administration of ketamine (1 to 2 mg/mouse), xylazine (170 to 340 μg/mouse), and acepromazine (30 to 60 μg/mouse), and treated with analgesics (local marcaine and systemic slow-release buprenorphine) as recommended by the CWRU Animal Resource Center veterinarians. An anterior incision was made from the patella to the proximal end of the right femur, and a unicortical pilot hole was made manually (0.75-mm pilot hole drill; KLS Martin, Jacksonville, FL) at the anterior medial aspect of

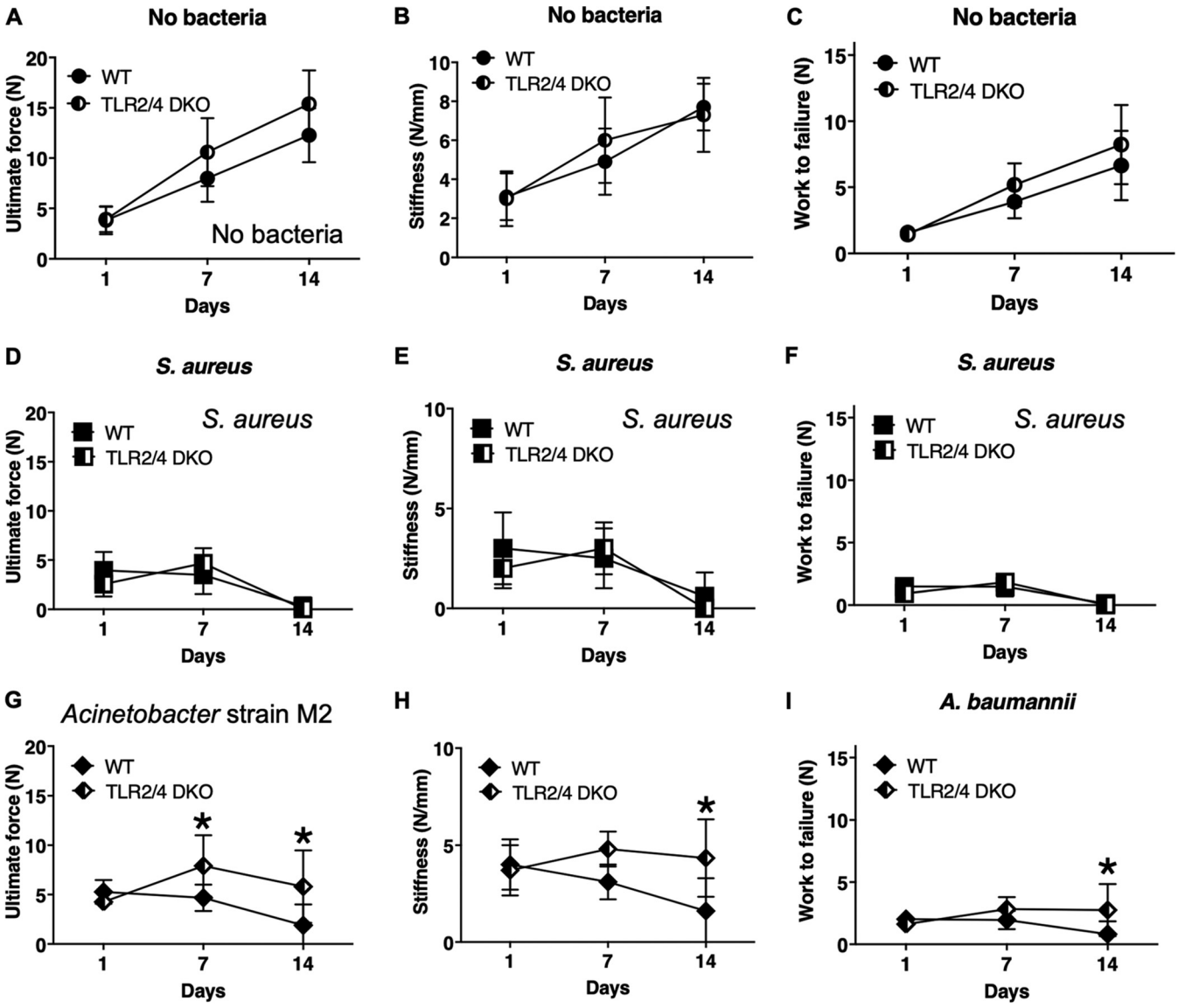

FIG 7 TLR2 and/or TLR4 mediate the effects of *Acinetobacter* strain M2 on osseointegration. Biomechanical measures of osseointegration in control groups without bacteria (A to C), in the high-dose *S. aureus* groups (D to F), and in the *Acinetobacter* strain M2 overnight incubation groups (G to I) were compared in TLR2$^{-/-}$;TLR4$^{-/-}$ mice and their wild-type (WT) control mice. *, $P < 0.05$ (parametric analysis). Error bars denote standard deviations. $n = 5$ to 9 mice/group.

the diaphysis (one-third of femoral length from the distal end). Implants were gently screwed through the pilot hole until contact was made with the opposite cortex (Fig. 2A). Muscles were allowed to return to the original position, and incisions were closed with sutures. In less than 5% of the mice, the femur fractured during implantation, and those mice were euthanized immediately. All other mice tolerated the surgery well and could ambulate immediately. Mice were euthanized by carbon dioxide inhalation followed by thoracotomy prior to histomorphometrical or biomechanical testing.

BLI. Bioluminescence (52) from anesthetized mice was measured 24 h before surgery as a baseline and longitudinally at the indicated time points after implant placement (Xenogen IVIS 200 system [Perkin Elmer/Caliper Life Sciences, Hopkinton, MA] in the CWRU Center for Imaging Research). Data were analyzed using Xenogen Living Image 2.5 (Perkin Elmer/Caliper Life Sciences). Oval regions of interest (ROI) of the same size were placed on the femoral region where the BLI signal originated for each mouse. BLI signals were quantified as the flux of photons within each ROI (photons/second) and reported after background subtraction.

Histomorphometry. Dissected femurs were fixed in formalin for 24 h and dehydrated in 70% ethanol. Histopathological preparation was performed in the CWRU Department of Orthopaedic's Hard Tissue Core Facility as described previously (56). Undecalcified ground cross sections (100 μm) were stained with Sanderson's rapid bone stain (Surgipath Medical Industries, Richmond, IL). This stain allows identification of osteoblasts, osteoclasts, osteoid, and mineralized bone in a single section (79). Because of the small size of the implants, it was possible to obtain only one central section of the implant per

mouse. Bone-to-implant contact and peri-implant bone were measured in a blinded manner using ImageJ analysis software (National Institutes of Health, Bethesda, MD). The bottom edge of the implant was excluded from all calculations (56).

Biomechanical testing. Pullout testing was performed immediately after euthanasia at a displacement rate of 1 mm/min as we described previously (52, 56). Pullout testing required approximately 3 min per mouse. Ultimate force, average stiffness, and work to failure were determined from load versus displacement curves according to ASTM standard F543-07. To reduce preloading variability, calculations of work began when force equaled 0.1 N.

To minimize the risk of bacterial cross-contamination during biomechanical testing, each day of testing was restricted to implants from either *S. aureus* or *Acinetobacter* strain M2 experiments. On each day of testing, the group of implants without bacteria were tested first, followed by the group with the lowest dose of bacteria, and then the groups of implants with progressively higher doses of bacteria. All grips and fixtures were sterilized with 70% ethanol between testing of each femur, and a new fixture assembly was used for each group of implants described in the previous sentence. After biomechanical testing, the same femurs were homogenized and each homogenate was subdivided for CFU counting, real-time PCR, and cytokine measurements (Fig. 1).

CFU counting and bacterial gene-specific real-time PCR. CFU and bacterial gene copies on implants and in surrounding femurs were quantified after pullout testing (52). Implants were sonicated for 10 min (50 W, 43,000 Hz) in PBS with 0.3% Tween 80, followed by vortexing for 5 min (50, 51). Femurs were homogenized in PBS (Pro200H; Pro Scientific, Oxford, CT) (50). CFU in sonicates and homogenates were counted on LB broth agar plates. DNA was extracted from sonicates and homogenates (Power Biofilm DNA isolation kit; MO BIO, Carlsbad, CA). Real-time PCR assays with primers that target the *S. aureus*-Xen36 *luxA* gene (5′-GACTTTCGCGTATTCGGCAC-3′ and 5′-ATTGAGCAGCCCACTCAGTC-3′; Primer-BLAST, National Center for Biotechnology Information) (52) or the *Acinetobacter* strain M2 *adeR* gene (5′-CACGCTAGCCATCCCATTGA-3′ and 5′-GCCTGAACTCTAGCGACCAC-3′) were quantified using the standard curve method as we described previously (80). Single peaks in melt curve analysis were confirmed in each assay.

Evaluation of proinflammatory cytokines and chemokine. For evaluation of proinflammatory cytokines and chemokine (52), femur homogenates were centrifuged (9,000 $\times$ *g*, 10 min) and supernatants were stored at −20°C. Concentrations of tumor necrosis factor alpha (TNF-α), IL-1β, IL-6, and CCL2 were measured with ELISA DuoSet minikits (catalog no. DY410, DY401, DY406, and DY479; R&D Systems, Minneapolis, MN).

Statistical analysis. Individual mice were the experimental unit for all statistical analyses (Prism 7; GraphPad Software, San Diego, CA). Power analysis using an alpha of 0.05 and a beta of 0.8 and our previous data in the murine implant infection model (52) found that the needed sample sizes were $n = 5$ or 6 for histomorphometry and $n = 8$ to 11 for biomechanical testing (SigmaStat; Systat Software, San Jose, CA). Sample sizes were adjusted based on data from the early experiments in the study. In experiments with more than three time points, statistical significance was determined by two-way analysis of variance (ANOVA), followed by Bonferroni's *post hoc* tests. In all other experiments, statistical significance was determined by Student's *t* test or one-way ANOVA, followed by Bonferroni's *post hoc* test in experiments with multiple groups. Nonparametric Mann-Whitney tests or Kruskal-Wallis analysis of variance followed by the Student-Newman-Keuls *post hoc* tests were applied to data sets that were not normally distributed or were not of equal variance. Normality was determined with the Shapiro-Wilks test, and variances were compared by F tests for experiments with two groups or by Bartlett's test for experiments with multiple groups (Prism 7; GraphPad Software). Tests were reported as significant if the *P* value was <0.05. Curve fitting was by quadratic regression analysis (Prism 7; GraphPad Software).

SUPPLEMENTAL MATERIAL

Supplemental material is available online only.

SUPPLEMENTAL FILE 1, PDF file, 0.4 MB.

ACKNOWLEDGMENTS

We thank Teresa Pizzuto for histological preparations, Nick Bernthal and Lloyd Miller for the homogenization protocol, Xin Chen for assistance with PCR, and Eric Pearlman for providing MAFIA mice.

This project was supported by a Department of Defense Peer Reviewed Orthopaedic Research Program Idea Development Award (E.M.G.), by the Mochida Memorial Foundation for Medical and Pharmaceutical Research (H.C.), and by the National Institute of Allergy and Infectious Diseases of the National Institutes of Health (grant no. R01AI072219 to R.A.B.). This study was supported in part by funds and/or facilities provided by the Cleveland Department of Veterans Affairs (award no. 1I01BX001974 to R.A.B.), by the Biomedical Laboratory Research & Development Service of the VA Office of Research and Development, and by the Geriatric Research Education and Clinical Center (VISN 10 to R.A.B.).

The content is solely the responsibility of the authors and does not necessarily represent the official views of the Department of Defense, the Mochida Memorial Foundation for

Medical and Pharmaceutical Research, the National Institutes of Health, or the Department of Veterans Affairs.

REFERENCES

1. Campoccia D, Montanaro L, Arciola CR. 2006. The significance of infection related to orthopedic devices and issues of antibiotic resistance. Biomaterials 27:2331–2339. https://doi.org/10.1016/j.biomaterials.2005.11.044.
2. Greenfield EM. 2014. Do genetic susceptibility, Toll-like receptors, and pathogen-associated molecular patterns modulate the effects of wear? Clin Orthop Relat Res 472:3709–3717. https://doi.org/10.1007/s11999-014-3786-4.
3. Ingham E, Fisher J. 2005. The role of macrophages in osteolysis of total joint replacement. Biomaterials 26:1271–1286. https://doi.org/10.1016/j.biomaterials.2004.04.035.
4. Danks L, Takayanagi H. 2013. Immunology and bone. J Biochem 154:29–39. https://doi.org/10.1093/jb/mvt049.
5. Wei S, Siegal GP. 2008. Mechanisms modulating inflammatory osteolysis: a review with insights into therapeutic targets. Pathol Res Pract 204:695–706. https://doi.org/10.1016/j.prp.2008.07.002.
6. Adamopoulos IE, Mellins ED. 2015. Alternative pathways of osteoclastogenesis in inflammatory arthritis. Nat Rev Rheumatol 11:189–194. https://doi.org/10.1038/nrrheum.2014.198.
7. Takayanagi H. 2015. SnapShot: osteoimmunology. Cell Metab 21:502.e1. https://doi.org/10.1016/j.cmet.2015.02.001.
8. Lacey DC, Simmons PJ, Graves SE, Hamilton JA. 2009. Proinflammatory cytokines inhibit osteogenic differentiation from stem cells: implications for bone repair during inflammation. Osteoarthritis Cartilage 17:735–742. https://doi.org/10.1016/j.joca.2008.11.011.
9. Graves DT, Oates T, Garlet GP. 2011. Review of osteoimmunology and the host response in endodontic and periodontal lesions. J Oral Microbiol 3:10.3402/jom.v3i0.5304. https://doi.org/10.3402/jom.v3i0.5304.
10. Sims NA. 2009. gp130 signaling in bone cell biology: multiple roles revealed by analysis of genetically altered mice. Mol Cell Endocrinol 310:30–39. https://doi.org/10.1016/j.mce.2008.08.025.
11. Nanes MS, Paciffici R. 2005. Inflammatory cytokines, p 67–90. *In* Bronner F, Farach-Carson MC, Rubin J (ed), Bone resorption. Springer-Verlag, London, United Kingdom. https://doi:10.1007/b136184.
12. Li YP, Stashenko P. 1992. Proinflammatory cytokines tumor necrosis factor-alpha and IL-6, but not IL-1, down-regulate the osteocalcin gene promoter. J Immunol 148:788–794.
13. Zhao L, Huang J, Zhang H, Wang Y, Matesic LE, Takahata M, Awad H, Chen D, Xing L. 2011. Tumor necrosis factor inhibits mesenchymal stem cell differentiation into osteoblasts via the ubiquitin E3 ligase Wwp1. Stem Cells 29:1601–1610. https://doi.org/10.1002/stem.703.
14. Thammasitboon K, Goldring SR, Boch JA. 2006. Role of macrophages in LPS-induced osteoblast and PDL cell apoptosis. Bone 38:845–852. https://doi.org/10.1016/j.bone.2005.10.013.
15. Bonsignore LA, Anderson JR, Lee Z, Goldberg VM, Greenfield EM. 2013. Adherent lipopolysaccharide inhibits the osseointegration of orthopedic implants by impairing osteoblast differentiation. Bone 52:93–101. https://doi.org/10.1016/j.bone.2012.09.011.
16. Branemark R, Branemark PI, Rydevik B, Myers RR. 2001. Osseointegration in skeletal reconstruction and rehabilitation: a review. J Rehabil Res Dev 38:175–181.
17. Kienapfel H, Sprey C, Wilke A, Griss P. 1999. Implant fixation by bone ingrowth. J Arthroplasty 14:355–368. https://doi.org/10.1016/s0883-5403(99)90063-3.
18. Hernandez CJ, Yang X, Ji G, Niu Y, Sethuraman AS, Koressel J, Shirley M, Fields MW, Chyou S, Li TM, Luna M, Callahan RL, Ross FP, Lu TT, Brito IL, Carli AV, Bostrom MPG. 2019. Disruption of the gut microbiome increases the risk of periprosthetic joint infection in mice. Clin Orthop Relat Res 477:2588–2598. https://doi.org/10.1097/CORR.0000000000000851.
19. Carli AV, Bhimani S, Yang X, Shirley MB, de Mesy Bentley KL, Ross FP, Bostrom MP. 2017. Quantification of peri-implant bacterial load and in vivo biofilm formation in an innovative, clinically representative mouse model of periprosthetic joint infection. J Bone Joint Surg Am 99:e25. https://doi.org/10.2106/JBJS.16.00815.
20. Thompson JM, Miller RJ, Ashbaugh AG, Dillen CA, Pickett JE, Wang Y, Ortines RV, Sterling RS, Francis KP, Bernthal NM, Cohen TS, Tkaczyk C, Yu L, Stover CK, DiGiandomenico A, Sellman BR, Thorek DL, Miller LS. 2018. Mouse model of Gram-negative prosthetic joint infection reveals therapeutic targets. JCI Insight 3:e121737. https://doi.org/10.1172/jci.insight.121737.
21. Heim CE, Vidlak D, Scherr TD, Kozel JA, Holzapfel M, Muirhead DE, Kielian T. 2014. Myeloid-derived suppressor cells contribute to Staphylococcus aureus orthopedic biofilm infection. J Immunol 192:3778–3792. https://doi.org/10.4049/jimmunol.1303408.
22. Niska JA, Meganck JA, Pribaz JR, Shahbazian JH, Lim E, Zhang N, Rice BW, Akin A, Ramos RI, Bernthal NM, Francis KP, Miller LS. 2012. Monitoring bacterial burden, inflammation and bone damage longitudinally using optical and muCT imaging in an orthopaedic implant infection in mice. PLoS One 7:e47397. https://doi.org/10.1371/journal.pone.0047397.
23. Wang Y, Cheng LI, Helfer DR, Ashbaugh AG, Miller RJ, Tzomides AJ, Thompson JM, Ortines RV, Tsai AS, Liu H, Dillen CA, Archer NK, Cohen TS, Tkaczyk C, Stover CK, Sellman BR, Miller LS. 2017. Mouse model of hematogenous implant-related Staphylococcus aureus biofilm infection reveals therapeutic targets. Proc Natl Acad Sci U S A 114:E5094–E5102. https://doi.org/10.1073/pnas.1703427114.
24. Vidlak D, Kielian T. 2016. Infectious dose dictates the host response during Staphylococcus aureus orthopedic-implant biofilm infection. Infect Immun 84:1957–1965. https://doi.org/10.1128/IAI.00117-16.
25. Yun HC, Branstetter JG, Murray CK. 2008. Osteomyelitis in military personnel wounded in Iraq and Afghanistan. J Trauma 64:S163–S168. https://doi.org/10.1097/TA.0b013e318160868c.
26. Fily F, Ronat JB, Malou N, Kanapathipillai R, Seguin C, Hussein N, Fakhri RM, Langendorf C. 2019. Post-traumatic osteomyelitis in Middle East war-wounded civilians: resistance to first-line antibiotics in selected bacteria over the decade 2006-2016. BMC Infect Dis 19:103. https://doi.org/10.1186/s12879-019-3741-9.
27. Johnson EN, Burns TC, Hayda RA, Hospenthal DR, Murray CK. 2007. Infectious complications of open type III tibial fractures among combat casualties. Clin Infect Dis 45:409–415. https://doi.org/10.1086/520029.
28. Petersen K, Riddle MS, Danko JR, Blazes DL, Hayden R, Tasker SA, Dunne JR. 2007. Trauma-related infections in battlefield casualties from Iraq. Ann Surg 245:803–811. https://doi.org/10.1097/01.sla.0000251707.32332.c1.
29. Dijkshoorn L, Nemec A, Seifert H. 2007. An increasing threat in hospitals: multidrug-resistant Acinetobacter baumannii. Nat Rev Microbiol 5:939–951. https://doi.org/10.1038/nrmicro1789.
30. Turton JF, Kaufmann ME, Gill MJ, Pike R, Scott PT, Fishbain J, Craft D, Deye G, Riddell S, Lindler LE, Pitt TL. 2006. Comparison of Acinetobacter baumannii isolates from the United Kingdom and the United States that were associated with repatriated casualties of the Iraq conflict. J Clin Microbiol 44:2630–2634. https://doi.org/10.1128/JCM.00547-06.
31. Scott P, Deye G, Srinivasan A, Murray C, Moran K, Hulten E, Fishbain J, Craft D, Riddell S, Lindler L, Mancuso J, Milstrey E, Bautista CT, Patel J, Ewell A, Hamilton T, Gaddy C, Tenney M, Christopher G, Petersen K, Endy T, Petruccelli B. 2007. An outbreak of multidrug-resistant Acinetobacter baumannii-calcoaceticus complex infection in the US military health care system associated with military operations in Iraq. Clin Infect Dis 44:1577–1584. https://doi.org/10.1086/518170.
32. Hujer KM, Hujer AM, Hulten EA, Bajaksouzian S, Adams JM, Donskey CJ, Ecker DJ, Massire C, Eshoo MW, Sampath R, Thomson JM, Rather PN, Craft DW, Fishbain JT, Ewell AJ, Jacobs MR, Paterson DL, Bonomo RA. 2006. Analysis of antibiotic resistance genes in multidrug-resistant Acinetobacter sp. isolates from military and civilian patients treated at the Walter Reed Army Medical Center. Antimicrob Agents Chemother 50:4114–4123. https://doi.org/10.1128/AAC.00778-06.
33. Morris FC, Dexter C, Kostoulias X, Uddin MI, Peleg AY. 2019. The mechanisms of disease caused by Acinetobacter baumannii. Front Microbiol 10:1601. https://doi.org/10.3389/fmicb.2019.01601.
34. Weber DJ, Rutala WA, Miller MB, Huslage K, Sickbert-Bennett E. 2010. Role of hospital surfaces in the transmission of emerging health care-associated pathogens: norovirus, Clostridium difficile, and Acinetobacter species. Am J Infect Control 38:S25–S33. https://doi.org/10.1016/j.ajic.2010.04.196.
35. Munoz-Price LS, Fajardo-Aquino Y, Arheart KL, Cleary T, DePascale D, Pizano L, Namias N, Rivera JI, O'Hara JA, Doi Y. 2013. Aerosolization of

Acinetobacter baumannii in a trauma ICU*. Crit Care Med 41:1915–1918. https://doi.org/10.1097/CCM.0b013e31828a39c0.
36. Spellberg B, Bonomo RA. 2013. "Airborne assault": a new dimension in Acinetobacter baumannii transmission*. Crit Care Med 41:2042–2044. https://doi.org/10.1097/CCM.0b013e31829136c3.
37. Munoz-Price LS, Weinstein RA. 2008. Acinetobacter infection. N Engl J Med 358:1271–1281. https://doi.org/10.1056/NEJMra070741.
38. Traglia GM, Place K, Dotto C, Fernandez JS, Montana S, Bahiense CDS, Soler-Bistue A, Iriarte A, Perez F, Tolmasky ME, Bonomo RA, Melano RG, Ramirez MS. 2019. Interspecies DNA acquisition by a naturally competent Acinetobacter baumannii strain. Int J Antimicrob Agents 53:483–490. https://doi.org/10.1016/j.ijantimicag.2018.12.013.
39. Ramirez MS, Bonomo RA, Tolmasky ME. 2020. Carbapenemases: transforming Acinetobacter baumannii into a yet more dangerous menace. Biomolecules 10:720. https://doi.org/10.3390/biom10050720.
40. Mortensen BL, Skaar EP. 2012. Host-microbe interactions that shape the pathogenesis of Acinetobacter baumannii infection. Cell Microbiol 14:1336–1344. https://doi.org/10.1111/j.1462-5822.2012.01817.x.
41. Feng Z, Jia X, Adams MD, Ghosh SK, Bonomo RA, Weinberg A. 2014. Epithelial innate immune response to Acinetobacter baumannii challenge. Infect Immun 82:4458–4465. https://doi.org/10.1128/IAI.01897-14.
42. Dou Y, Song F, Guo F, Zhou Z, Zhu C, Xiang J, Huan J. 2017. Acinetobacter baumannii quorum-sensing signalling molecule induces the expression of drug-resistance genes. Mol Med Rep 15:4061–4068. https://doi.org/10.3892/mmr.2017.6528.
43. Lin L, Tan B, Pantapalangkoor P, Ho T, Baquir B, Tomaras A, Montgomery JI, Reilly U, Barbacci EG, Hujer K, Bonomo RA, Fernandez L, Hancock RE, Adams MD, French SW, Buslon VS, Spellberg B. 2012. Inhibition of LpxC protects mice from resistant Acinetobacter baumannii by modulating inflammation and enhancing phagocytosis. mBio 3:e00312-12. https://doi.org/10.1128/mBio.00312-12.
44. Zurawski DV, Banerjee J, Alamneh YA, Shearer JP, Demons ST. 2019. Skin and soft tissue models for Acinetobacter baumannii infection. Methods Mol Biol 1946:271–287. https://doi.org/10.1007/978-1-4939-9118-1_25.
45. Jacobs AC, Thompson MG, Black CC, Kessler JL, Clark LP, McQueary CN, Gancz HY, Corey BW, Moon JK, Si Y, Owen MT, Hallock JD, Kwak YI, Summers A, Li CZ, Rasko DA, Penwell WF, Honnold CL, Wise MC, Waterman PE, Lesho EP, Stewart RL, Actis LA, Palys TJ, Craft DW, Zurawski DV. 2014. AB5075, a highly virulent isolate of Acinetobacter baumannii, as a model strain for the evaluation of pathogenesis and antimicrobial treatments. mBio 5:e01076-14. https://doi.org/10.1128/mBio.01076-14.
46. Collinet-Adler S, Castro CA, Ledonio CG, Bechtold JE, Tsukayama DT. 2011. Acinetobacter baumannii is not associated with osteomyelitis in a rat model: a pilot study. Clin Orthop Relat Res 469:274–282. https://doi.org/10.1007/s11999-010-1488-0.
47. Crane DP, Gromov K, Li D, Soballe K, Wahnes C, Buchner H, Hilton MJ, O'Keefe RJ, Murray CK, Schwarz EM. 2009. Efficacy of colistin-impregnated beads to prevent multidrug-resistant A. baumannii implant-associated osteomyelitis. J Orthop Res 27:1008–1015. https://doi.org/10.1002/jor.20847.
48. Gieling F, Peters S, Erichsen C, Richards RG, Zeiter S, Moriarty TF. 2019. Bacterial osteomyelitis in veterinary orthopaedics: pathophysiology, clinical presentation and advances in treatment across multiple species. Vet J 250:44–54. https://doi.org/10.1016/j.tvjl.2019.06.003.
49. Guarch-Perez C, Riool M, Zaat SA. 2021. Current osteomyelitis mouse models, a systematic review. Eur Cell Mater 42:334–374. https://doi.org/10.22203/eCM.v042a22.
50. Bernthal NM, Stavrakis AI, Billi F, Cho JS, Kremen TJ, Simon SI, Cheung AL, Finerman GA, Lieberman JR, Adams JS, Miller LS. 2010. A mouse model of post-arthroplasty Staphylococcus aureus joint infection to evaluate in vivo the efficacy of antimicrobial implant coatings. PLoS One 5:e12580. https://doi.org/10.1371/journal.pone.0012580.
51. Pribaz JR, Bernthal NM, Billi F, Cho JS, Ramos RI, Guo Y, Cheung AL, Francis KP, Miller LS. 2012. Mouse model of chronic post-arthroplasty infection: noninvasive in vivo bioluminescence imaging to monitor bacterial burden for long-term study. J Orthop Res 30:335–340. https://doi.org/10.1002/jor.21519.
52. Choe H, Narayanan AS, Gandhi DA, Weinberg A, Marcus RE, Lee Z, Bonomo RA, Greenfield EM. 2015. Immunomodulatory peptide IDR-1018 decreases implant infection and preserves osseointegration. Clin Orthop Relat Res 473:2898–2907. https://doi.org/10.1007/s11999-015-4301-2.
53. Niu C, Clemmer KM, Bonomo RA, Rather PN. 2008. Isolation and characterization of an autoinducer synthase from Acinetobacter baumannii. J Bacteriol 190:3386–3392. https://doi.org/10.1128/JB.01929-07.
54. Carruthers MD, Harding CM, Baker BD, Bonomo RA, Hujer KM, Rather PN, Munson RS. Jr, 2013. Draft genome sequence of the clinical isolate Acinetobacter nosocomialis strain M2. Genome Announc 1:e00905-13. https://doi.org/10.1128/genomeA.00906-13.
55. Yadav A, Saini V, Arora S. 2010. MCP-1: chemoattractant with a role beyond immunity: a review. Clin Chim Acta 411:1570–1579. https://doi.org/10.1016/j.cca.2010.07.006.
56. Bonsignore LA, Colbrunn RW, Tatro JM, Messerschmitt PJ, Hernandez CJ, Goldberg VM, Stewart MC, Greenfield EM. 2011. Surface contaminants inhibit osseointegration in a novel murine model. Bone 49:923–930. https://doi.org/10.1016/j.bone.2011.07.013.
57. Duan Y, Beck TJ, Wang XF, Seeman E. 2003. Structural and biomechanical basis of sexual dimorphism in femoral neck fragility has its origins in growth and aging. J Bone Miner Res 18:1766–1774. https://doi.org/10.1359/jbmr.2003.18.10.1766.
58. de Breij A, Eveillard M, Dijkshoorn L, van den Broek PJ, Nibbering PH, Joly-Guillou ML. 2012. Differences in Acinetobacter baumannii strains and host innate immune response determine morbidity and mortality in experimental pneumonia. PLoS One 7:e30673. https://doi.org/10.1371/journal.pone.0030673.
59. Bruhn KW, Pantapalangkoor P, Nielsen T, Tan B, Junus J, Hujer KM, Wright MS, Bonomo RA, Adams MD, Chen W, Spellberg B. 2015. Host fate is rapidly determined by innate effector-microbial interactions during Acinetobacter baumannii bacteremia. J Infect Dis 211:1296–1305. https://doi.org/10.1093/infdis/jiu593.
60. Eveillard M, Soltner C, Kempf M, Saint-Andre JP, Lemarie C, Randrianarivelo C, Seifert H, Wolff M, Joly-Guillou ML. 2010. The virulence variability of different Acinetobacter baumannii strains in experimental pneumonia. J Infect 60:154–161. https://doi.org/10.1016/j.jinf.2009.09.004.
61. Dikshit N, Kale SD, Khameneh HJ, Balamuralidhar V, Tang CY, Kumar P, Lim TP, Tan TT, Kwa AL, Mortellaro A, Sukumaran B. 2018. NLRP3 inflammasome pathway has a critical role in the host immunity against clinically relevant Acinetobacter baumannii pulmonary infection. Mucosal Immunol 11:257–272. https://doi.org/10.1038/mi.2017.50.
62. Li D, Gromov K, Soballe K, Puzas JE, O'Keefe RJ, Awad H, Drissi H, Schwarz EM. 2008. Quantitative mouse model of implant-associated osteomyelitis and the kinetics of microbial growth, osteolysis, and humoral immunity. J Orthop Res 26:96–105. https://doi.org/10.1002/jor.20452.
63. Croes M, van der Wal BCH, Vogely HC. 2019. Impact of bacterial infections on osteogenesis: evidence from in vivo studies. J Orthop Res 37:2067–2076. https://doi.org/10.1002/jor.24422.
64. Cassat JE, Hammer ND, Campbell JP, Benson MA, Perrien DS, Mrak LN, Smeltzer MS, Torres VJ, Skaar EP. 2013. A secreted bacterial protease tailors the Staphylococcus aureus virulence repertoire to modulate bone remodeling during osteomyelitis. Cell Host Microbe 13:759–772. https://doi.org/10.1016/j.chom.2013.05.003.
65. Glowacki J, Mizuno S, Kung J, Goff J, Epperly M, Dixon T, Wang H, Greenberger JS. 2014. Effects of mouse genotype on bone wound healing and irradiation-induced delay of healing. In Vivo 28:189–196.
66. Pajarinen J, Jamsen E, Konttinen YT, Goodman SB. 2014. Innate immune reactions in septic and aseptic osteolysis around hip implants. J Long Term Eff Med Implants 24:283–296. https://doi.org/10.1615/jlongtermeffmedimplants.2014010564.
67. Glucksam-Galnoy Y, Sananes R, Silberstein N, Krief P, Kravchenko VV, Meijler MM, Zor T. 2013. The bacterial quorum-sensing signal molecule N-3-oxo-dodecanoyl-L-homoserine lactone reciprocally modulates pro- and anti-inflammatory cytokines in activated macrophages. J Immunol 191:337–344. https://doi.org/10.4049/jimmunol.1300368.
68. Kale SD, Dikshit N, Kumar P, Balamuralidhar V, Khameneh HJ, Bin Abdul Malik N, Koh TH, Tan GGY, Tan TT, Mortellaro A, Sukumaran B. 2017. Nod2 is required for the early innate immune clearance of Acinetobacter baumannii from the lungs. Sci Rep 7:17429. https://doi.org/10.1038/s41598-017-17653-y.
69. Qiu H, KuoLee R, Harris G, Van Rooijen N, Patel GB, Chen W. 2012. Role of macrophages in early host resistance to respiratory Acinetobacter baumannii infection. PLoS One 7:e40019. https://doi.org/10.1371/journal.pone.0040019.
70. Yajjala VK, Thomas VC, Bauer C, Scherr TD, Fischer KJ, Fey PD, Bayles KW, Kielian T, Sun K. 2016. Resistance to acute macrophage killing promotes airway fitness of prevalent community-acquired Staphylococcus aureus strains. J Immunol 196:4196–4203. https://doi.org/10.4049/jimmunol.1600081.
71. Hanke ML, Heim CE, Angle A, Sanderson SD, Kielian T. 2013. Targeting macrophage activation for the prevention and treatment of Staphylococcus aureus

biofilm infections. J Immunol 190:2159–2168. https://doi.org/10.4049/jimmunol.1202348.
72. Wagner C, Obst U, Hansch GM. 2005. Implant-associated posttraumatic osteomyelitis: collateral damage by local host defense? Int J Artif Organs 28:1172–1180. https://doi.org/10.1177/039139880502801115.
73. Greenfield EM, Bi Y, Ragab AA, Goldberg VM, Van De Motter RR. 2002. The role of osteoclast differentiation in aseptic loosening. J Orthop Res 20:1–8. https://doi.org/10.1016/S0736-0266(01)00070-5.
74. Trevors JT. 2012. Can dead bacterial cells be defined and are genes expressed after cell death? J Microbiol Methods 90:25–28. https://doi.org/10.1016/j.mimet.2012.04.004.
75. Choe H, Inaba Y, Kobayashi N, Aoki C, Machida J, Nakamura N, Okuzumi S, Saito T. 2013. Use of real-time polymerase chain reaction for the diagnosis of infection and differentiation between gram-positive and gram-negative septic arthritis in children. J Pediatr Orthop 33:e28-33–e33. https://doi.org/10.1097/BPO.0b013e318279c6b6.
76. Choe H, Aota Y, Kobayashi N, Nakamura Y, Wakayama Y, Inaba Y, Saito T. 2014. Rapid sensitive molecular diagnosis of pyogenic spinal infections using methicillin-resistant Staphylococcus-specific polymerase chain reaction and 16S ribosomal RNA gene-based universal polymerase chain reaction. Spine J 14:255–262. https://doi.org/10.1016/j.spinee.2013.10.044.
77. Hise AG, Daehnel K, Gillette-Ferguson I, Cho E, McGarry HF, Taylor MJ, Golenbock DT, Fitzgerald KA, Kazura JW, Pearlman E. 2007. Innate immune responses to endosymbiotic Wolbachia bacteria in Brugia malayi and Onchocerca volvulus are dependent on TLR2, TLR6, MyD88, and Mal, but not TLR4, TRIF, or TRAM. J Immunol 178:1068–1076. https://doi.org/10.4049/jimmunol.178.2.1068.
78. Greenfield EM, Beidelschies MA, Tatro JM, Goldberg VM, Hise AG. 2010. Bacterial pathogen-associated molecular patterns stimulate biological activity of orthopaedic wear particles by activating cognate Toll-like receptors. J Biol Chem 285:32378–32384. https://doi.org/10.1074/jbc.M110.136895.
79. Sanderson C. 1997. Entering the realm of mineralized bone processing: a review of the literature and techniques. J Histotechnol 20:259–266. https://doi.org/10.1080/01478885.1997.11878769.
80. Dai JC, He P, Chen X, Greenfield EM. 2006. TNFalpha and PTH utilize distinct mechanisms to induce IL-6 and RANKL expression with markedly different kinetics. Bone 38:509–520. https://doi.org/10.1016/j.bone.2005.10.007.